



HAL
open science

Artificial recharge of aquifers and pumping: transient analytical solutions for hydraulic head and impact on streamflow rate based on the spatial superposition method

Benoît Dewandel, Sandra Lanini, Vivien Hakoun, Yvan Caballero,
Jean-Christophe Maréchal

► To cite this version:

Benoît Dewandel, Sandra Lanini, Vivien Hakoun, Yvan Caballero, Jean-Christophe Maréchal. Artificial recharge of aquifers and pumping: transient analytical solutions for hydraulic head and impact on streamflow rate based on the spatial superposition method. *Hydrogeology Journal*, 2021, 29 (3), pp.1009-1026. 10.1007/s10040-020-02294-9. hal-03154763

HAL Id: hal-03154763

<https://brgm.hal.science/hal-03154763>

Submitted on 1 Mar 2021

HAL is a multi-disciplinary open access archive for the deposit and dissemination of scientific research documents, whether they are published or not. The documents may come from teaching and research institutions in France or abroad, or from public or private research centers.

L'archive ouverte pluridisciplinaire **HAL**, est destinée au dépôt et à la diffusion de documents scientifiques de niveau recherche, publiés ou non, émanant des établissements d'enseignement et de recherche français ou étrangers, des laboratoires publics ou privés.

1 **Artificial recharge of aquifers and pumping: transient analytical solutions for hydraulic**
2 **head and impact on streamflow rate based on the spatial superposition method**

3 Benoît Dewandel^{1,2} & Sandra Lanini^{1,2} & Vivien Hakoun^{1,2} & Yvan Caballero^{1,2} & Jean-
4 Christophe Maréchal^{1,2}

5 1 BRGM, Univ Montpellier, Montpellier, France

6 2 G-eau, UMR 183, INRAE, CIRAD, IRD, AgroParisTech, Supagro, BRGM, Montpellier,
7 France

8 * Corresponding author

9 **Abstract**

10 The behaviour of a transient groundwater mound in response to infiltration from surface
11 basins has been studied for at least the past 80 years. Although analytical solutions are known
12 for a large variety of situations, some common settings still lack a solution.

13 We remind and show that integrating the line-sink solution developed for pumping an
14 unconfined aquifer by Hantush (1964a; 1965), considering the surface of the recharging area,
15 is identical to his well-known solution for groundwater mounding below a rectangular basin
16 (Hantush, 1967). This implies from a general standpoint that the principle of superposition
17 can be used for directly implementing pumping wells, as well as aquifer boundaries, to a
18 unique solution. Moreover, we show that other line-sink solutions, provided that partial
19 differential equations behaviour is linear, can be used with a spatial superposition method for
20 addressing a variety of hydrogeological settings.

21 Based on this trivial principle and on existing line-sink solutions, we propose several
22 analytical solutions able to consider a rectangular recharging area and a pumping well in an
23 unconfined aquifer: (i) near a stream, (ii) between a stream and a no-flow boundary, with and
24 without the influence of natural recharge, (iii) near a stream that partially penetrates the
25 aquifer and (iv) for a multi-layer aquifer. For cases including streams, transient solutions of
26 the impact on streamflow rate are also established.

27 The proposed analytical solutions will be useful applications for Managed Aquifer Recharge,
28 in particular the design of structures for artificially recharging an aquifer, possibly pumped by
29 one or several wells.

30 Key words: groundwater mounding, pumping, stream, layered aquifer, analytical solutions,
31 Managed Aquifer Recharge.

32 **1. Introduction**

33 Managed Aquifer Recharge (MAR) with surface water or treated wastewater, through
34 trenches, basins, wells, dammed streams, canals, etc., is commonly used for limiting water-
35 table decline, storing surface or storm water, controlling seawater intrusion, reducing land
36 subsidence, or improving the quality of the injected water through geopurification (e.g.,
37 Bouwer, 2002; Aish, 2010; Ganot et al., 2017). MAR based on systems such as basins, dams,
38 and specific irrigation practices (Yihdego, 2017), is used for enhancing groundwater resources
39 in regions facing water scarcity because of limited precipitation and/or where aquifers are
40 over-exploited (e.g., Dillon, 2005; Dillon et al., 2009; Bhuiyan, 2015; Massuel et al., 2014;
41 Boisson et al., 2014, Lee et al., 2015; Stafford et al., 2015; Kacimov et al., 2016, Nicolas et
42 al., 2019).

43 Before constructing MAR systems, their future efficiency must be evaluated, which requires
44 fieldwork and drilling, monitoring of ground and surface water, and knowledge of aquifer
45 properties (Dillon, 2005). Before starting detailed investigations and their subsequent
46 modelling, analytical models can be used for a preliminary assessment of MAR opportunities.
47 Such an assessment would be useful for different purposes, such as siting and pre-designing
48 the recharging structures, assessing the groundwater mounding, evaluating the amount of
49 water that can be stored and, finally, assess the impact of the MAR on nearby streams.

50 Since the early 1950s, several analytical solutions were developed for defining the growth and
51 decay of groundwater mounds. These solutions consider infiltration from rectangular or
52 circular basins with constant or transient recharging rates (Baumann, 1952; Glover, 1960;
53 Hantush, 1967; Hunt, 1971; Marino, 1975; Latinopoulos, 1981; Warner et al., 1989; Rao and
54 Sarma, 1981, Rai and Singh, 1996; Rai et al., 1998, 2001). For most of these solutions, flow
55 from the recharge basin is assumed to be horizontal (Dupuit-Forchheimer assumption),
56 occurring through an infinite, uniform and isotropic aquifer. Several authors evaluated these
57 solutions against numerical modelling (e.g., Warner et al. 1989; Carleton, 2010) and showed
58 that the seminal solution given by Hantush (1967) -one of the most widely used and cited
59 (Finnemore, 1995; Zomorodi, 2005)- is very accurate. This solution assumes an infinite,
60 unconfined, isotropic and horizontal aquifer (with Dupuit-Forchheimer assumption), and was
61 obtained from an approximation of the Boussinesq partial differential equation (linearized
62 form see Appendix A-1) by means of Laplace transform (Hantush, 1964a, b, 1967).
63 Additional solutions were developed for considering other boundary conditions; these
64 included a recharging area in aquifers with no-flow and constant-head boundaries (Marino,

65 1974; Rao and Sarma, 1981, 1984; Latinopoulos, 1984; Molden et al., 1984; Manglik et al.,
66 1997), or pumping wells near the MAR structure (Manglik et al., 2004). A recent solution also
67 considered sloping aquifers (Zlotnik et al., 2017). Carleton (2010) conducted numerical
68 experiments for evaluating the effect of vertical anisotropy in hydraulic conductivity on the
69 shape of mounding; his results showed that the greater the horizontal hydraulic conductivity
70 (i.e. $K_h/K_v > 1$), the more the height of mounding by classical analytical solutions (e.g.
71 Hantush, 1967) will be underestimated.

72 Existing works present analytical solutions for tackling complex hydrogeological settings, but
73 some common settings still lack a solution. Such settings include, for example, assessment of
74 the impact of MAR on a stream where an infiltration basin and pumping wells are located
75 between the stream and a no-flow boundary, with or without natural recharge. Others are
76 where infiltration basins and pumping wells are located close to a clogged stream, or the case
77 of a multi-layer aquifer system.

78 We first remind and demonstrate that the Hantush (1967) solution can be found by integrating
79 the line sink solution developed for pumping-test interpretation in an unconfined aquifer
80 (Hantush, 1964a, 1965) over the surface of the recharging area. Then, based on existing line
81 sink solutions and the application of the principle of superposition because of the linear
82 property of partial differential equations, we present and discuss solutions where the aquifer is
83 space-limited (Dirichlet's and/or no-flow boundary conditions), where a stream partially
84 penetrates the aquifer, and for a multi-layer aquifer system. Theoretical cases (Fig. 1) are
85 presented for a recharging area and a pumping well in four unconfined aquifer settings: i) an
86 aquifer near a river (Fig. 1a); ii) an aquifer with a river and a no-flow boundary (strip aquifer),
87 with and without the influence of natural recharge (Fig. 1b); iii) an aquifer near a stream with
88 a clogged streambed that partially penetrates the aquifer (Fig. 1c); and iv) a recharging top-
89 layer aquifer and pumping at the bottom of a semi-confined aquifer (Fig. 1d). In addition, we
90 provide approximate but useful transient solutions for evaluating the impact of MAR (in terms
91 of flow rate) on the stream, for the presented cases.

92

93 Our study seeks alternative transient analytical solutions based on the spatial superposition
94 method for computing groundwater mounding (or depletion), or its impact on a stream while
95 recharging and pumping unconfined aquifers. These solutions are useful and could be
96 implemented in operational tools for engineers designing recharge structures, and/or

97 improving the management of existing MAR structures. We do not suggest that the proposed
 98 solutions should replace existing analytical or numerical models used for modelling
 99 groundwater mounding. Rather, they are meant to supplement existing models for improving
 100 the design of such engineered systems.

101

102 2. Mathematical statements

103 Assuming an unconfined, infinite and horizontal aquifer, characterized by constant and
 104 uniform hydraulic conductivity and storativity (storage coefficient), and that groundwater
 105 flow is horizontal (Dupuit-Forchheimer assumption), Hantush (1964a, b, 1965) obtained an
 106 analytical solution of the hydraulic head for a well pumping in such an aquifer, from a
 107 linearized form of the Boussinesq equation (Appendix A-2) and by using Laplace transform.
 108 In this solution, the well is vertical, fully penetrates the aquifer and is pumped with a constant
 109 pumping rate Q_{Pump} (here $Q_{Pump} < 0$). Because of the Hantush's linearization (see Hantush,
 110 1964a, b; 1965), the solution is applicable only when the declining levels with respect to the
 111 initial water-table depth do not exceed one-half of the initial aquifer thickness (ie: $h_0 -$
 112 $h < 0.5h_0$). The transient evolution of hydraulic head at a location x_{obs}, y_{obs} can be deduced
 113 from:

$$114 \quad Z_{Pump}(x_{obs}, y_{obs}, t) = h^2 - h_0^2 = \frac{Q_{Pump}}{2\pi K} W\left(\frac{r^2}{4vt}\right) \quad (1)$$

115 with h_0 the initial hydraulic head, h (or $h(x_{obs}, y_{obs}, t)$) the hydraulic head at t , $v = \frac{K\bar{b}}{S}$, the
 116 diffusivity, $r = \sqrt{x_{obs}^2 + y_{obs}^2}$, the distance to the pumping well, K the hydraulic
 117 conductivity of the aquifer and S the aquifer storativity. $W(u)$ is the well-function (or
 118 exponential integral, $E_1(u)$), \bar{b} is a constant of linearization that can be approximated by the
 119 average aquifer thickness at the point of interest ($\bar{b} = \frac{1}{2}(h_0 + h_t)$) and t the period at the end
 120 of which h is to be evaluated (Hantush, 1965; Warner et al.1989). Usually, \bar{b} is estimated after
 121 several successive iterations (Hantush, 1967; Marino, 1967). Note that Eq. 1 is identical to the
 122 Theis solution (Theis, 1935) for a fully penetrating well in a confined isotropic aquifer, where
 123 drawdown is small in comparison to the aquifer thickness ($h_0 - h \ll h_0$), with S here being the
 124 aquifer storage coefficient and \bar{b} the aquifer thickness (in this case $\bar{b} = \text{constant}$).

125 Because of the linear behaviour of the Hantush partial differential equation and assuming that
 126 the percolating water directly enters the aquifer (absence of vadose zone), Eq. 1 can be

127 integrated into a rectangular surface to give a solution of groundwater mounding for a
 128 rectangular basin (Fig.2). Therefore, with a total recharging rate Q_{Rech} ($Q_{Rech}>0$) the
 129 integration of Eq. 1 leads to the following expression:

$$Z_{Rech}(x_{obs}, y_{obs}, t) = h^2 - h_o^2 = \frac{1}{2\pi K} \int_{-x_L}^{+x_L} \int_{-y_L}^{+y_L} \frac{Q_{Rech}}{4x_L y_L} W \left(\frac{(x - x_{obs})^2 + (y - y_{obs})^2}{4vt} \right) dx dy$$

(2)

131 Where $2x_L$ and $2y_L$ characterize the rectangular recharging area lengths along the x -axis and
 132 the y -axis respectively. $x=y=0$ at the centre of the rectangle.

133 Assuming that the recharging rate, R , is uniformly distributed on the rectangular recharging
 134 area ($2x_L \times 2y_L$), Q_{Rech} can be expressed as a function of R ($R = \frac{Q_{Rech}}{4x_L y_L}$), and it is shown that
 135 Eq. 2 is identical to the analytical solution of groundwater mounding for a rectangular basin
 136 with a uniform percolation rate (Fig.2), proposed by Hantush (1967); Eq. 3. Appendix B
 137 presents the demonstration. Note that the demonstration exposed in appendix presents
 138 similarities to that presented in Polubarinova-Kochina book (1977) and the one used for
 139 modelling drawdown of a pumping test in a well that intersects fractures (Dewandel et al.,
 140 2018).

$$Z_{Rech}(x_{obs}, y_{obs}, t) = h^2 - h_o^2 = \frac{R\bar{b}}{2S} \int_0^t \left[\text{Erf} \left(\frac{x_L + x_{obs}}{2\sqrt{v\tau}} \right) + \text{Erf} \left(\frac{x_L - x_{obs}}{2\sqrt{v\tau}} \right) \right] \times \left[\text{Erf} \left(\frac{y_L + y_{obs}}{2\sqrt{v\tau}} \right) + \text{Erf} \left(\frac{y_L - y_{obs}}{2\sqrt{v\tau}} \right) \right] d\tau$$

(3)

142 Assumptions and mathematical hypothesis of Eq. 3 are the same as the ones exposed before
 143 (see also Hantush 1967): unconfined, infinite and horizontal aquifer; Dupuit-Forchheimer
 144 assumption, the solution is a valid for $h-h_o < 0.5h_o$ and the infiltrating water directly enters the
 145 aquifer. Aquifer parameters are defined before.

146 Though ‘mathematically trivial’, these solutions can be easily used or combined for a large
 147 variety of hydrogeological settings based on mainly four interesting points. First, as already
 148 suggested by Hantush (1967), the principle of superposition (image-well theory) can be used
 149 with Eq. 3 for defining aquifer boundaries. For example, Molden et al. (1984) used this
 150 principle for modelling groundwater mounding from a rectangular basin near a stream, using
 151 Glover’s (1960) analytical solution. However, their solution assumes that the mound’s height

152 is negligible compared to the initial saturated thickness (ie, $h-h_0 \approx h_0$), which is not the case
 153 here. Second, it is possible to combine Z pumping terms (Z_{Pump} in Eq. 1) and recharging areas
 154 (Z_{Rech} in Eq. 3)—and, by extension, aquifer boundaries—in a unique analytical solution for
 155 computing hydraulic head where recharging area and pumping wells are located in a space-
 156 limited aquifer, such as between a river (using Dirichlet’s condition) and a no-flow boundary.
 157 Third, Equation 1 can be integrated over any surface geometry (not necessarily a rectangle or
 158 a circle) and aquifer boundaries (if any) need not to be parallel or perpendicular to the basin
 159 geometry. Fourth and last, other line-sink solutions can be applied to consider other aquifer
 160 settings, provided that corresponding governing partial differential equation is linear and the
 161 use of the spatial superposition method. A similar theoretical approach was used by Zlotnik et
 162 al. (2017), who estimated the groundwater mounding of a rectangular basin in a sloping
 163 aquifer from the appropriate well solution (Hantush, 1964a, b). However, as Molden et al.
 164 (1984), their solution assumes that the mound’s height is negligible compared to the initial
 165 saturated thickness and no solution including aquifer limits or stream was proposed.

166 Applying this principle of superposition, we propose alternative settings including a stream
 167 that partially penetrates the aquifer and a multi-layer aquifer system. In the following, Z
 168 terms and other integrals were evaluated using the Gauss-Legendre quadrature.

169

170 **3. Theoretical examples with a stream fully penetrating the aquifer**

171 *3.1 Solutions for a rectangular recharging area and a pumping well near a stream*

172 3.1.1. Hydraulic-head solution

173 As noted above and because of the linear behaviour of the partial differential equation, an
 174 analytical solution can be obtained using the principle of superposition (image-well theory,
 175 Ferris et al., 1962; Kruseman and de Ridder, 1994; Dewandel et al., 2014) for a rectangular
 176 recharging area and a pumping well near a stream; Figs. 1a and 3a). The aquifer is unconfined
 177 and horizontal, and characterized by its hydraulic conductivity (K) and its storativity (S), and
 178 the stream fully penetrates the aquifer (constant-head boundary or Dirichlet’s condition). For
 179 simplicity, the solution being provided in Z terms, the hydraulic-head solution can be deduced
 180 from the following expression:

181

$$\underbrace{\hspace{10em}}_{\text{Real 'recharge'}} \quad \underbrace{\hspace{10em}}_{\text{Imaginary 'recharge'}}$$

$$\underbrace{\hspace{20em}}_{\hspace{20em}} \quad \underbrace{\hspace{20em}}_{\hspace{20em}}$$

208 For the recharge area, since the hydraulic-head solution for a rectangular recharging area is
 209 identical to the integration of the well solution for an unconfined aquifer over the same area,
 210 the superposition principle is still valid for evaluating the impact on the stream with Eq. 6a.
 211 Therefore:

$$\Delta q_{Rech} = \int_{-x_L}^{+x_L} \int_{-y_L}^{+y_L} \frac{Q_{rech}}{4x_L y_L} \operatorname{Erfc} \left(\sqrt{\frac{S(d-x)^2}{4Kh_0 t}} \right) dx dy = \int_{-x_L}^{+x_L} \frac{Q_{rech}}{2x_L} \operatorname{Erfc} \left(\sqrt{\frac{S(d-x)^2}{4Kh_0 t}} \right) dx$$

(6b)

214 An approximation of this solution can be obtained, if the x -length of the rectangular
 215 recharging area is small compared to the distance between recharging area and stream (d -
 216 $x_L \gg 2x_L$, in practice a ratio of five is enough). Therefore, Eq. 6b becomes the solution
 217 provided by Glover and Balmer (1954):

$$\Delta q_{Rech} = Q_{rech} \operatorname{Erfc} \left(\sqrt{\frac{Sd^2}{4Kh_0 t}} \right)$$

(6c)

219 with $Q_{Rech} = 4x_L y_L R$ ($Q_{Rech} > 0$); R the uniform infiltration rate.

220 The approximate form of Eq. 5 can now be written as:

$$\Delta q = \Delta q_{Rech} + \Delta q_{Pump} = Q_{rech} \operatorname{Erfc} \left(\sqrt{\frac{Sd^2}{4Kh_0 t}} \right) + Q_{Pump} \operatorname{Erfc} \left(\sqrt{\frac{S(d-x_w)^2}{4Kh_0 t}} \right)$$

(7)

222 which is easier to manipulate and of interesting practical use, as it allows adding as many
 223 terms as there are recharging areas and pumping wells.

224 Figure 4b shows computations of the impact on the stream for the settings described on
 225 figures 1a and 3a. Aquifer parameters are the same as in Figure 4a. As expected, the
 226 integration of a hydraulic-head gradient along the stream (Eq. 5) and the approximate solution
 227 (Eq. 7) give similar results. These results show that over short times (<10 days) the
 228 streamflow rate is reduced because of the short distance between well and stream. Over longer
 229 times (>20 days), the contribution of the recharging area becomes noticeable and the
 230 depletion flow-rate reduces, the impact on the stream reducing over time. By contrast, when

231 the pumping well is located on the other side of the recharging area ($x_w=-140$ m), the
 232 behaviour is reversed. After a short time, most water comes from the recharging area and
 233 streamflow increases. Then, the flow rate decreases because of the impact of the pumping
 234 well on the stream. However, in both cases, the equilibrium—nil influence on the stream as
 235 $Q_{Pump}=Q_{rech}$ (i.e. $\overline{Q_{Rech}} = -\overline{Q_{Pump}}$)—will be reached only after a very long time. When
 236 considering one recharging area and one pumping well, a nil impact right from the start of
 237 recharging and pumping occurs where these systems are equidistant from the stream (cf.
 238 Eq. 7).

239 *3.2 Solutions for a rectangular recharging area and a pumping well between a stream and a*
 240 *no-flow boundary*

241 3.2.1. Hydraulic-head solution

242 A solution for the hydraulic head for a rectangular recharging area and a pumping well
 243 between two parallel boundaries can also be found using the superposition principle, still
 244 because of the linearity of partial differential equation (e.g. Dewandel et al., 2014). Therefore,
 245 a generic solution for both terms (i.e. recharging area and pumping well) can be used for
 246 computing the hydraulic head in this setting:

$$\begin{aligned}
 Z_{2Limit} = Z + & \sum_{n=0,2,4..}^{\infty} b^{n/2+1} c^{n/2} Z(2nL + 2d - x_{obs}, y_{obs}, t) + \sum_{n=2,4..}^{\infty} (bc)^{n/2} Z(-2nL - x_{obs}, y_{obs}, t) \\
 & + \sum_{n=2,4..}^{\infty} (bc)^{n/2} Z(2nL - x_{obs}, y_{obs}, t) + \sum_{n=2,4..}^{\infty} b^{n/2-1} c^{n/2} Z(-(2nL - 2d) - x_{obs}, y_{obs}, t)
 \end{aligned}
 \tag{8a}$$

247
 248 where b and c are coefficients associated with each boundary, b or $c=1$ for a no-flow
 249 boundary, and b or $c=-1$ for a constant-head boundary (stream, i.e Dirichlet's condition); d is
 250 the distance between the centre of the recharging area and the stream, and $2L$ is the distance
 251 between both limits (Fig. 3b), $x=y=0$ at the centre of the recharging area. For the pumping
 252 well, x_{obs} has to be replaced by $x_{obs}-x_w$, y_{obs} by $y_{obs}-y_w$, and d by $d-x_w$; x_w and y_w are coordinates
 253 of the pumping well. For the case of a rectangular recharging area, and a pumping well
 254 between a stream and a no-flow boundary, $b=-1$ and $c=1$. Note that this solution can be used
 255 for two parallel no-flow boundaries ($b=c=1$) or two streams ($b=c=-1$). To solve Eq.8a (but
 256 also the following Eqs.9), we used an algorithm based on an iterative process, where the
 257 number of images is defined when the absolute value given by the n^{th} computation becomes
 258 negligible. In the presented case (Fig.4c), computations were stopped when the value is lower

259 than 4.10^{-7} , which corresponds to 15 image wells. This criterion insures a high accuracy of
 260 computation.

261 As for the previous case, the aquifer is unconfined and horizontal, and characterized by its
 262 hydraulic conductivity (K), its storativity (S), and the solution is a valid for $|h-h_0| < 0.5h_0$.

263 The hydraulic-head solution can now be found from:

264

$$h^2 - h_0^2 = Z_{2Limit_Rech} + Z_{2Limit_Pump} \quad (8b)$$

265

266 where Z_{2Limit_Rech} , refers to the component of the recharging rectangular area and Z_{2Limit_Pump} to
 267 the pumping well. Both expanded expressions are given in Appendix C.

268 Figure 4c gives examples of hydraulic-head computations with Equation 8b. Aquifer
 269 parameters, distance to stream, infiltration rate, pumping location and flow rate are identical
 270 to the previous case (Fig. 4a). The no-flow boundary is located at 400 m from the centre of
 271 the recharging area, creating a 700 m-wide strip aquifer. Hydraulic-head computations were
 272 done with and without pumping from the well after 60 days of recharging and pumping.
 273 Compared to the example without a no-flow boundary (Fig. 4a), the hydraulic head is slightly
 274 higher everywhere for the case without pumping. With an active pumping well, the head is
 275 slightly higher west of the recharging area, and slightly lower because of pumping to the east.

276 3.2.2. Impact of recharging area and pumping well on streamflow rate

277 As above, the impact on streamflow can be evaluated either from Eq. 5, or separately. For the
 278 pumping well, the impact on stream flow is given by Lelièvre (1969):

$$\Delta q_{Pump} = Q_{Pump} \left[\operatorname{Erfc} \left(\sqrt{\frac{S(d-x_w)^2}{4Kh_0t}} \right) + \sum_{n=1,2,3..}^{\infty} (-1)^n \left(\operatorname{Erfc} \left(\frac{4nL + (d-x_w)}{2\sqrt{Kh_0t/S}} \right) - \operatorname{Erfc} \left(\frac{4nL - (d-x_w)}{2\sqrt{Kh_0t/S}} \right) \right) \right] \quad (9a)$$

279

280 For the recharging area and using the same development as in the previous case, an
 281 approximate solution can be found, if $(d-x_L) \gg 2x_L$. It takes a similar form:

$$\Delta q_{Rech} = Q_{Rech} \left[\operatorname{Erfc} \left(\sqrt{\frac{Sd^2}{4Kh_0t}} \right) + \sum_{n=1,2,3..}^{\infty} (-1)^n \left(\operatorname{Erfc} \left(\frac{4nL+d}{2\sqrt{Kh_0t/S}} \right) - \operatorname{Erfc} \left(\frac{4nL-d}{2\sqrt{Kh_0t/S}} \right) \right) \right]$$

282

(9 b)

283 Under this condition, the impact on streamflow results from the sum of the two components in
 284 a form like Eq. 7 ($\Delta q = \Delta q_{Rech} + \Delta q_{Pump}$). This form is also easier to manipulate and allows
 285 adding as many terms as there are recharging areas and pumping wells.

286 Figure 4d shows computations of the impact on stream flow for the setting described on
 287 Figure 4c. The aquifer parameters are the same as in Figure 4a. As before, the integration of a
 288 hydraulic-head gradient along the stream (Eq. 5) and the approximate solution
 289 (Eq. 9a+Eq. 9b) are in good agreement. The impact on streamflow, for a pumping well
 290 located east of the recharging area, or one to the west between the recharge area and the no-
 291 flow boundary, is similar to that on Figure 4b: river depletion linked to the pumping well and
 292 flow towards the river linked to the recharging area, respectively. However, compared to the
 293 semi-finite aquifer, the relaxation time is shorter and a quasi-steady-state is reached earlier
 294 because of the limited extent of the aquifer.

295 3.2.3. Steady-state solution of hydraulic head for an infinite strip aquifer along the y-axis,
 296 limited by a river and a no-flow boundary: the case of natural recharging

297 In this case, $b=-1$ and $c=1$, $2x_L=2L$, $d=L$, $y_L \rightarrow \infty$ and $t \rightarrow \infty$ (steady-state) in the solution for the
 298 recharging area (Eq. C-2). Figure 5a shows the computation of hydraulic heads for natural
 299 recharge only. Aquifer parameters, distance to stream and distance to no-flow boundary are
 300 identical to those on Figure 4c. We consider a uniform distribution of natural recharge (R) at a
 301 rate of 1.27×10^{-8} m/s (i.e. 400 mm/year). The solution is the same as that of Bruggeman
 302 (1999; sol. 21.11, p. 24; and Eq. 10, below), which corresponds to the hydraulic-head profile
 303 for a steady-state condition caused by recharge from precipitation (R) through an infinite strip
 304 of width $2L$, bounded on one side by a stream and on the other by a no-flow boundary. The
 305 error to Bruggeman's solution is very low (standardized root mean square error: 1.3×10^{-5}).
 306 Other tests are presented in Appendix C. Even for the extreme case of a very thin aquifer
 307 ($h_0=1.5$ m; Appendix C), we found very consistent results, with little differences probably
 308 linked to numerical error (standardized Root Mean Square Error $< 2 \times 10^{-5}$). Furthermore, the
 309 small errors prove that the numerical evaluation of the integrals is accurate.

310 Consequently, for a long time span (i.e. steady-state; $t \rightarrow \infty$), the solution tends to:

$$Z_{NaturalRech} = h^2 - h_o^2 = \frac{R}{K}(4L^2 - (x + L)^2) \quad (10)$$

311

312 with $x=0$ at the centre of the strip.

313 To include a mean annual aquifer recharge with artificial recharging areas and pumping wells,
 314 Eq. 10 can be combined with Eq. 8b, providing an analytical solution for the hydraulic head in
 315 the hydrogeological setting presented above ($h^2 - h_o^2 = Z_{LimitRech} + Z_{LimitPump} +$
 316 $Z_{NaturalRech}$). The impact on the stream of the recharging structure and the pumping well, can
 317 also be evaluated from Eq. 5, but both are identical to the previous case (Eqs. 9a, b) because
 318 of the superposition theory. Figure 5b shows an example with a recharging area and a
 319 pumping well at 140 m from the centre of the recharging area, after 1 day and 60 days of
 320 recharging and pumping. All other parameters are the same as above (Figure 4c).

321

322 4. Theoretical examples for other aquifer settings

323 Here we explore how other line-sink solutions can consider other aquifer settings, provided
 324 that governing partial differential equations are linear. For a pumping well, a generic solution
 325 of hydraulic head is given by:

$$Z_{Pump}(x_{obs}, y_{obs}, t) = h^2 - h_o^2 = \frac{Q_{Pump}}{2\pi K} f(x_{obs}, y_{obs}, t, \bar{b}, \alpha, \beta, \gamma \dots) \quad (11a)$$

326

327 where $f(x_{obs}, y_{obs}, t, \bar{b}, \alpha, \beta, \gamma \dots)$ is a line-sink solution, for example an existing analytical solution
 328 for a well pumping a specific unconfined aquifer defined by parameters $\alpha, \beta, \gamma \dots$, with
 329 $Q_{Pump} < 0$.

330 For a rectangular recharging area—but this is applicable to all surface geometry—and
 331 assuming a uniform percolation rate, Eq. 2 can be generalized using spatial superposition
 332 method as follows:

$$Z_{Rech}(x_{obs}, y_{obs}, t) = h^2 - h_o^2 = \frac{R}{2\pi K} \int_{-x_L}^{+x_L} \int_{-y_L}^{+y_L} f(x_{obs}, y_{obs}, t, \bar{b}, \alpha, \beta, \gamma \dots) dx dy \quad (11b)$$

333

334 Eq. 11b may have an analytical form, or it can be evaluated numerically (e.g. by Gauss-
 335 Legendre quadrature). Combined with Eq. 11a, one obtains the solution for a setting where
 336 artificial recharge takes place through a rectangular area and pumping from a well. Because of
 337 the linearization of partial differential equations, the solution is a valid for $h-h_0 < 0.5h_0$. In the
 338 following, no boundary condition were implemented, therefore $h(\pm\infty, y, t) = h(x, \pm\infty, t) = h_0$ (or
 339 $Z(\pm\infty, y, t) = Z(x, \pm\infty, t) = 0$).

340

341 *4.1. Solutions for partial stream penetration and a partially clogged streambed*

342 *4.1.1. Hydraulic-head solution*

343 The solutions are derived from Hunt's (1999) analytical solutions. In this conceptual model
 344 (Fig. 1c), the groundwater flux is assumed to be horizontal (Dupuit-Forchheimer assumption),
 345 the aquifer is unconfined, infinite and horizontal, and characterized by its hydraulic
 346 conductivity and storativity. This solution assumes that streambed penetration of the aquifer
 347 and dimensions of the streambed cross section are all relatively small compared to aquifer
 348 thickness, and that stream level is constant and maintained at the initial groundwater level
 349 (i.e., h_0). It also assumes that the streambed is partially clogged and that a linear relationship
 350 exists between the seepage rate through the streambed and the change in hydraulic head
 351 across the semi-pervious clogging layer.

352 *4.1.2. Hydraulic-head solution*

353 Assuming the linearized form of the Boussinesq equation as in Hantush (1967), for an
 354 unconfined aquifer, and after a change of variables (see Appendix D), Hunt's (1999) solution
 355 for hydraulic head and for a pumping well, expressed in term of Z , can be re-written as
 356 follows:

$$\begin{aligned}
 Z_{\text{HuntPump}}(x_{\text{obs}}, y_{\text{obs}}, t) &= h^2 - h_0^2 \\
 &= \frac{Q_{\text{Pump}}}{2\pi K} \left[W\left(\frac{x_{\text{obs}}^2 + y_{\text{obs}}^2}{4vt}\right) - \int_0^1 W\left(\frac{(d + |d - x_{\text{obs}}| - 2K\bar{b}Ln(u)/\lambda)^2 + y_{\text{obs}}^2}{4vt}\right) du \right]
 \end{aligned}$$

357 (12a)

358 with $\lambda = \frac{b}{b''}k''$; b is the stream width, b'' the streambed thickness, k'' the streambed hydraulic
 359 conductivity, and Q_{Pump} (<0) the pumping flow-rate. Here, $x=y=0$ at the pumping well. Note
 360 that when $\lambda \rightarrow 0$ (i.e. impervious streambed), Eq. 12a gives Eq.1; and also when $\lambda \rightarrow \infty$ (stream

361 fully penetrating the aquifer), Eq. 12a gives the hydraulic-head solution for a pumping well
 362 near a stream with zero drawdown (Theis, 1941; Glover and Balmer, 1954; see also § 3.1.1.).

363 According to the demonstration given in section 2, the hydraulic-head solution for a
 364 rectangular recharging area can be found by integrating Eq. 12a into the rectangular area
 365 ($2x_L \times 2y_L$). Therefore, we obtain:

$$\begin{aligned}
 Z_{\text{HuntRect}}(x_{\text{obs}}, y_{\text{obs}}, t) &= h^2 - h_o^2 \\
 &= \frac{R\bar{b}}{2S} \left\{ \int_0^t \left[\text{Erfc} \left(\frac{x_L + x_{\text{obs}}}{2\sqrt{v\tau}} \right) + \text{Erfc} \left(\frac{x_L - x_{\text{obs}}}{2\sqrt{v\tau}} \right) \right] \times \left[\text{Erfc} \left(\frac{y_L + y_{\text{obs}}}{2\sqrt{v\tau}} \right) + \text{Erfc} \left(\frac{y_L - y_{\text{obs}}}{2\sqrt{v\tau}} \right) \right] d\tau \right. \\
 &\quad - \int_0^t \int_0^1 \left[\text{Erfc} \left(\frac{x_L + (d + |d - x_{\text{obs}}| + 2K\bar{b}Ln(u)/\lambda)}{2\sqrt{v\tau}} \right) \right. \\
 &\quad \left. \left. + \text{Erfc} \left(\frac{x_L - (d + |d - x_{\text{obs}}| + 2K\bar{b}Ln(u)/\lambda)}{2\sqrt{v\tau}} \right) \right] \times \left[\text{Erfc} \left(\frac{y_L + y_{\text{obs}}}{2\sqrt{v\tau}} \right) \right. \right. \\
 &\quad \left. \left. + \text{Erfc} \left(\frac{y_L - y_{\text{obs}}}{2\sqrt{v\tau}} \right) \right] dud\tau \right\}
 \end{aligned}$$

366 (12b)

367 with $x=y=0$ at the centre of the recharging area.

368 As mentioned before, this solution also assumes that the percolating water directly enters the
 369 aquifer (no vadose zone). Therefore, the sum of both Z terms, similar to Eq. 8 ($h^2 - h_o^2 =$
 370 $Z_{\text{HuntRect}} + Z_{\text{HuntPump}}$), gives the hydraulic-head solution for a rectangular recharging area
 371 and a pumping well located near a partially clogged stream. As before, the solution assumes
 372 that the decline, or rise, of the groundwater mound in case of recharging, should not exceed
 373 one-half of the initial saturated thickness ($|h-h_0| < 0.5h_0$).

374 4.1.3. Impact of recharging area and pumping well on stream flow rate

375 According to Hunt (1999), the impact on a stream is given by:

$$\Delta q = \lambda \int_{-\infty}^{+\infty} h(d, y, t) dy$$

376 (13a)

377 and can also be evaluated separately for the pumping well (Hunt, 1999) as:

$$\Delta q_{\text{HuntPump}} = Q_{\text{Pump}} \left[\text{Erfc} \left(\sqrt{\frac{S(d-x_w)^2}{4K\bar{b}t}} \right) - e^{\left(\frac{\lambda^2 t}{4SK\bar{b}} + \frac{\lambda(d-x_w)}{2K\bar{b}} \right)} \text{Erfc} \left(\sqrt{\frac{\lambda^2 t}{4SK\bar{b}t}} + \sqrt{\frac{S(d-x_w)^2}{4K\bar{b}t}} \right) \right]$$

378

(13b)

379 For the rectangular recharging area, an approximate solution can also be given if $(d-x_L) \gg 2x_L$
 380 for the impact on the stream. It takes a similar form, while replacing $d-x_w$ by d and Q_{Pump} by
 381 Q_{Rech} ($Q_{\text{Rech}} = 4x_L y_L$) in Eq. 13b. Eq. 13a, with the appropriate solution for h , can also be
 382 used. Therefore, an approximate solution involving a recharging area and a pumping well is
 383 also found, taking a similar form as the previous cases (i.e., $\Delta q = \Delta q_{\text{RechHunt}} +$
 384 $\Delta q_{\text{PumpHunt}}$).

385 Figures 6a and b give computation examples of hydraulic head and impact on streamflow rate
 386 for the aquifer setting described above, with various stream leakance values ($\lambda = \infty, 10^{-4}, 5 \cdot 10^{-5},$
 387 $10^{-5}, 5 \cdot 10^{-6}$ and 10^{-6} m/s), the stream being 10 m wide. Aquifer properties are identical to
 388 previous examples ($K=10^{-4}$ m/s, $S=0.05$, $h_0=12$ m) and the stream is offset 300 m from the
 389 centre of the recharging area ($x_L=y_L=40$ m, $R=2.96 \times 10^{-6}$ m/s). The pumping well is located
 390 between the stream and the recharging area, 140 m from the centre of the latter. The
 391 recharging area and pumping well have equal injection/pumping rate ($Q_{\text{Rech}}=Q_{\text{Pump}}=17$ m³/h).
 392 For $\lambda = \infty$, the hydraulic head profile and its impact on the stream are, as expected, identical to
 393 Eq. 4 (stream fully penetrating the aquifer). For lower λ values the clogging increases and
 394 stream-aquifer exchanges are reduced, the hydraulic head being lower near the stream.
 395 Consequently, the impact on streamflow rate is lowered and delayed as λ decreases (Fig. 6b).
 396 This figure also shows that the approximate solution for evaluating the impact on the stream
 397 (Eq. 13b, with $\Delta q = \Delta q_{\text{RechHunt}} + \Delta q_{\text{PumpHunt}}$) is in good agreement with Eq. 13a.

398

399 4.2. Solutions for a rectangular recharging area and a pumping well in a multi-aquifer system

400 In this last case, we consider a recharging area on top of a multi-layer aquifer (Fig. 1d). The
 401 recharging area feeds an unconfined aquifer layer and pumping occurs in the deeper semi-
 402 confined layer. Recharging of the top layer induces a rise in hydraulic head in the deeper
 403 layer, but pumping there induces depletion in the upper layer. The system is characterized by

404 an upper aquifer with hydraulic conductivity K_1 and storage coefficient (or storativity) S_1 , and
405 a deeper aquifer with transmissivity T_2 and storage coefficient S_2 . The aquifers are separated
406 by an aquitard of hydraulic conductivity k' and thickness e' . Horizontal flow is assumed in
407 both aquifers. The line-sink solutions for this conceptual model are extensions of the Hunt and
408 Scott (2007) two-aquifer model.

409 For the given example (Figs. 7a, b, c), $K_1=10^{-4}$ m/s, $S_1=0.05$ and $h_0=12$ m are identical to
410 previous cases, as are $T_2=10^{-4}$ m²/s, $S_2=10^{-3}$ and ratio $k'/e'=5 \times 10^{-7}$ s⁻¹. The recharging area and
411 pumping distances are the same as before. Figures 7a and b are two examples of hydraulic-
412 head profiles at $t=1$ day and $t=60$ days in the top unconfined layer (Fig. 7a), and drawdown or
413 rise in the deeper layer (Fig. 7b). A comparison between our solution and Hantush's one with
414 a pumping well (Eq. 4 with $K=10^{-4}$ m/s, $h_0=12$ m, $S=0.05$ and $d \rightarrow \infty$) reveals that, near the
415 recharging area, hydraulic heads from our solution are lower than Hantush's. This difference
416 stems from the percolation of water towards the deeper aquifer layer (Fig. 7b). The recharging
417 area induces a rise of water levels in the deep aquifer of up to 0.7 m at $t=1$ day and up to
418 1.1 m at $t=60$ days. Hydraulic heads in the top aquifer layer are impacted by the well pumping
419 from the deeper layer; these heads are depleted by up to 0.6 m and 1.4 m after $t=1$ day and 60
420 days, respectively.

421 To evaluate the flow rate entering the deeper aquifer layer, we computed the accumulated
422 volume that was abstracted/recharged up to a given time from/into each aquifer. This
423 computation was done by integrating the difference in hydraulic head in the x-y plane of the
424 top layer, multiplying this difference by the aquifer storativity, and subtracting the resulting
425 volume from the volume of water added by recharging. Finally, a vertical drainage rate was
426 computed for the entire system and compared to the rate stemming from the recharging area
427 only (without pumping).

428 In the example shown on Fig. 7c, recharging and pumping rates are identical. Drainage results
429 not only from the recharging area (top layer) to the deeper layer, but also from pumping the
430 deep layer (percolation from the top layer). Over longer times, the computed drainage rate
431 (16.6 m³/h) almost counterbalances the pumping rate from the deeper aquifer layer
432 (17.0 m³/h). However, comparing this result to the situation where there is only a recharging
433 area (without pumping well) shows that drainage rate from the recharging area to the deeper
434 aquifer layer is minor (0.4 m³/h). This shows that pumping in the deeper layer has a greater
435 drainage effect on the top aquifer layer because of the large cone of depression induced by

436 pumping, than the water infiltrating from the top layer and recharging the deep aquifer. In the
437 latter case, only a small amount of water infiltrated by the recharging basin benefits the
438 pumping well.

439

440 **5. Discussion and Conclusions**

441 The integration of the line-sink solution developed for unconfined aquifers (Hantush, 1964a,
442 b, 1965) over the surface of a recharging area is mathematically identical to the well-known
443 solution of Hantush (1967). The latter solution allows characterizing the rise and decline of a
444 groundwater mound in response to uniform infiltration from a rectangular basin, obtained
445 from a linearized form of the Boussinesq equation and Laplace transform (see the text for
446 mathematical assumptions). This is a consequence of the linearity of the partial differential
447 equation, and implies that the principle of superposition can be used to directly implement
448 aquifer boundaries, as earlier suggested by Hantush (1967), as well as pumping wells.

449 Therefore, analytical solutions for hydraulic head are first proposed for two common
450 hydrogeological settings: (i) a rectangular recharging area and a pumping well near a stream
451 (Dirichlet's condition), and (ii) a rectangular recharging area and a pumping well between a
452 stream and a no-flow boundary. We show that, under steady-state conditions, the analytical
453 solution developed for the second setting is equivalent to Bruggeman's (1999) solution for a
454 hydraulic-head profile resulting from recharge over an infinite strip bounded on one side by a
455 stream and on the other side by a no-flow boundary. Therefore, a solution is proposed for the
456 hydrogeological setting (ii) and the influence of natural recharge.

457 We also propose transient solutions for evaluating the impact on streamflow rate of a
458 recharging area and a pumping well. Even though, rigorously, the impact must be computed
459 by integrating the hydraulic gradient along the stream (Eq. 5), we demonstrate that
460 approximate solutions provide accurate results that can be used in most cases, as long as the
461 distance from the side of the recharging area to the stream is small in comparison to the x -
462 length of the recharging area. Such approximate solutions are identical to the existing
463 analytical solution for evaluating the impact of a pumping well on a stream (e.g., Glover and
464 Balmer, 1954; Lelièvre, 1969), and can be combined for separately evaluating the impacts
465 from the recharging area and the pumping well. From a practical viewpoint, these solutions
466 can be used with any number of recharging areas and pumping wells. In the given examples,
467 where infiltration and pumping rates are equal, equilibrium, i.e. nil impact on streamflow rate,

468 was not reached even after one year. This result shows that managed artificial recharge design
469 must account for transient behaviour, and that the location of recharging areas and pumping
470 wells must be carefully considered to avoid streamflow rate depletion, or contrarily that a
471 significant part of the recharging water percolates straight into the stream.

472 We also propose a generic analytical solution for modelling transient hydraulic head in more
473 complex aquifer settings with impact on streamflow rates, based on the integration of
474 solutions over the recharging area. This provides the possibility of using other line-sink
475 solutions for considering other aquifer settings, provided that governing partial differential
476 equations are linear. We first derived from Hunt (1999) a solution involving a rectangular
477 recharging area and a pumping well near a stream (with a clogged streambed) that partially
478 penetrates the aquifer. Our results show that the solution proposed by Hunt (1999) for
479 evaluating the impact of a pumping well on a stream, also appears to be a good approximation
480 for evaluating the impact of a recharging area.

481 An example for a multi-layer aquifer, with and without a pumping well, is also given. . The
482 solution computes hydraulic head in both layers, while recharging and pumping the upper and
483 deeper layers, respectively. This solution allows evaluating the rise and/or decline of water
484 levels in both layers, as well as evaluating the vertical drainage flow-rate between the upper
485 and deeper layers. In the example shown, the impact on the deeper aquifer of the recharging
486 area in terms of vertical drainage is lower than the impact of pumping the deeper aquifer on
487 the near-surface layer, illustrating that only little water infiltrating from the basin really
488 benefits the deeper aquifer.

489 Impacts on streamflow rate are given for the whole stream, but it may be of interest to
490 evaluate it over a particular length. This can be achieved with Eq. 5 or Eq. 13a while
491 integrating solutions for the appropriate interval. The total volume of stream depletion or rise
492 over a certain time, can be evaluated by integrating the flow-rate solution over that period.
493 Analytical solutions for the cases presented on Figures 2 and 3 can be found, e.g., in Hantush
494 (1965) and Lelièvre (1969). We also consider that other existing analytical solutions, obtained
495 for stream depletion created by a well on other aquifer settings (e.g. Hunt, 2014), may be
496 valid approximate solutions for evaluating the impact of recharging areas.

497 Recharging or pumping-rate variations, not considered here, can also be incorporated using
498 the principle of superposition on Z terms (e.g. Hantush, 1967). The solutions developed here
499 are applicable when the rise or decline in the unconfined aquifer is less than one-half of the

500 initial saturated aquifer thickness ($|h-h_0| < 0.5h_0$, h_0 being the initial hydraulic head). However,
501 investigations by Marino (1967) with similar analytical expressions showed that they give
502 good results, even when the water table rise is much larger than the initial saturated thickness.
503 This is consistent with the trials presented in Appendix C. Finally, the proposed solutions
504 assume that the percolating water directly enters the aquifer. Extensions to account for non-
505 instantaneous drainage from the vadose zone above the water table could be considered using
506 Moench's (1996) solution.

507 In conclusion, the generic solution proposed above develops valid solutions for any surface
508 geometry, not necessarily rectangular or circular, and for aquifer boundaries that are not
509 necessarily parallel or at right angle to the basin geometry. In addition, the solution helps
510 testing a large panel of hydrogeological settings, including a stream flowing on the top layer
511 of a multi-layer aquifer that is recharged and pumped (with the solutions of Hunt, 2009), or
512 where only the deep layer is pumped (Ward and Lough, 2011), or an aquifer that is recharged
513 and where pumping takes place through a fracture (Dewandel et al., 2018). Future works
514 should also focus on unconfined and anisotropic aquifers, with the problem that in this case
515 hydraulic head depends on depth (Neuman, 1975).

516

517 **Acknowledgements**

518 This study was conducted by BRGM, and was funded by the internal BRGM RDI Recharging
519 project and the 'Dem'Eaux Roussillon' project funded by BRGM, European Funds for
520 Regional Development, Rhone Mediterranean & Corsica Water Agency, Communauté
521 urbaine Perpignan Méditerranée Métropole and the Pyrenées Orientales Department. The two
522 anonymous Journal referees are thanked for their useful remarks and comments that improved
523 the quality of the paper. We are grateful to Dr. H.M. Kluijver for revising the final version of
524 the English text. A patent application has been deposited on parts of this work (French
525 National Institute of Industrial Property).

526

527 **References**

- 528 Aish, A.M., 2010. Simulation of groundwater mound resulting from proposed artificial
529 recharge of treated sewage effluent case study – Gaza waste water treatment plan, Palestine.
530 *Geologia Croatica*, 62-73. doi: 104154/gc.2010.04
- 531 Baumann, P., 1952, Groundwater movement controlled through spreading: Transactions,
532 American Society of Civil Engineers, v. 117, p. 1024–1060.
- 533 Bhuiyan, C., 2015. An approach towards site selection for water banking in unconfined
534 aquifers through artificial recharge. *Journal of Hydrology*, 523, 465–474.
535 <http://dx.doi.org/10.1016/j.jhydrol.2015.01.052>.
- 536 Boisson, A., Baïssat, M., Alazard, M., Perrin, J., Villesseche, D., Dewandel, B., Kloppmann,
537 W., Chandra, S., Picot-Colbeaux, G., Sarah, S., Ahmed, S., Maréchal, J.-C., 2014.
538 Comparison of surface and groundwater balance approaches in the evaluation of managed
539 aquifer recharge structures: Case of a percolation tank in a crystalline aquifer in India. *Journal*
540 *of Hydrology*, 519, 1620–1633. <http://dx.doi.org/10.1016/j.jhydrol.2014.09.022>.
- 541 Bouwer, H., 2002. Artificial recharge of groundwater: hydrogeology and engineering.
542 *Hydrogeology Journal*, 10, 121–142. DOI 10.1007/s10040-001-0182-4.
- 543 Bruggeman, G.A., 1999. Analytical Solutions of Geohydrological Problems. *Developments in*
544 *Water Science* 46, Elsevier, The Netherlands, 959 p.
- 545 Carleton, G.B., 2010. Simulation of groundwater mounding beneath hypothetical stormwater
546 infiltration basins: U.S. Geological Survey Scientific Investigations Report 2010-5102, 64 p.
- 547 Dewandel, B., Lanini, S., Lachassagne, P., Maréchal, J.C., 2018. A generic analytical solution
548 for modelling pumping tests in wells intersecting fractures. *Journal of Hydrology*, 559, 89–99,
549 <https://doi.org/10.1016/j.jhydrol.2018.02.013>
- 550 Dewandel, B., Aunay, B., Maréchal, J.C., Roques, C., Bour, O., Mougin, B., Aquilina, L.,
551 2014. Analytical solutions for analysing pumping tests in a sub-vertical and anisotropic fault
552 zone draining shallow aquifers. *Journal of Hydrology* , 509, 115–131.
- 553 Dillon, P., 2005. Future management of aquifer recharge, *Hydrogeological Journal*, 13, 313–
554 316, <https://doi.org/10.1007/s10040-004-0413-6>, 2005.
- 555 Dillon, P.J., Gale, I., Contreras, S., Pavelic, P., Evans, R., Ward, J., 2009. Managing aquifer
556 recharge and discharge to sustain irrigation livelihoods under water scarcity and climate
557 change. Retrieved from. IAHS-AISH Publication 330 (September), 1–12.
- 558 Ferris, J.G., Knowles, D.B., Brown, R.H., Stallman, R.W., 1962. Theory of aquifer tests. U.S.
559 Geological Survey Water-Supply Paper, 69–174.
- 560 Finnemore, E.J., 1995. A program to calculate ground-water mound heights: *Ground Water*,
561 33, 139–143.
- 562 Ganot, Y., Holtzman, R., Weisbrod, N., Nitzan, I., Katz, Y., Kurtzman, D., 2017. Monitoring
563 and modeling infiltration–recharge dynamics of managed aquifer recharge with desalinated
564 seawater. *Hydrol. Earth Syst. Sci.*, 21, 4479–4493. <https://doi.org/10.5194/hess-21-4479-2017>

- 565 Glover, R.E., 1960, Mathematical derivations as pertain to groundwater recharge: Fort
566 Collins, Colorado, U.S. Department of Agriculture Agricultural Research Service, 81 p.
- 567 Glover, R.E., Balmer, C.G., 1954. River depletion from pumping a well near a river.
568 Transactions of the American Geophysical Union, 35(3), 468–470.
- 569 Hantush, M.S., 1964a. Hydraulics of Wells. *In* Advances in Hydrosience. v.1, ed. V.T.
570 Chow. Academic Press.
- 571 Hantush, M.S., 1964b. Depletion of storage, leakage, and river flow by gravity wells in
572 sloping sands. Journ. of Geophys. Research, 69 (12), 2551-2560.
- 573 Hantush, M.S., 1965. Wells near streams with semipervious beds. Journal of Geophysical
574 Research, 70 (12), 2829-2838.
- 575 Hantush, M.S., 1967, Growth and decay of groundwater mounds in response to uniform
576 percolation: Water Resources Research, 3, 227–234.
- 577 Hunt, B.W., 1971, Vertical recharge of unconfined aquifers: Journal of Hydraulic Division,
578 American Society of Civil Engineers, 97, no. HY7, 1017–1030.
- 579 Hunt, B., 1999. Unsteady stream depletion from ground water pumping. Ground Water, 37(1),
580 98–102.
- 581 Hunt, B., 2009. Stream depletion in a two-layer leaky aquifer system. Journal of Hydrological
582 Engineering, 10.1061/(ASCE)HE.1943-5584.0000063, 895–903.
- 583 Hunt, B., 2014. Review of stream depletion solutions, behavior, and calculations. Journal of
584 Hydrological Engineering, 10.1061/(ASCE)HE.1943-5584.0000768, 167-178.
- 585 Hunt, B., Scott D., 2007. Flow to a well in a two-aquifer system. Journal of Hydrological
586 Engineering, 10.1061/(ASCE)1084-0699(2007)12:2(146), 146–155.
- 587 Kacimov, A., Zlotnik, R.V., Al-Maktoumi, A., Al-Abri, R., 2016. Modeling of transient water
588 table response to managed aquifer recharge: A lagoon in Muscat, Oman. Environmental Earth
589 Sciences 75, 4: 318. DOI:<https://doi.org/10.1007/s12665-015-5137-5>.
- 590 Kruseman, G.P., de Ridder, N.A., 1994. Analysis and evaluation of pumping test data. ILRI
591 publication 47. Wageningen, The Netherlands.
- 592 Latinopoulos, P., 1981. The response of groundwater on artificial recharges schemes. Water
593 Resources Research, 17(6), 1712-1714.
- 594 Latinopoulos, P., 1984. Periodic recharge to finite aquifers from rectangular areas. Adv.
595 Water Resources, 7, 137-140.
- 596 Lee, H., Koo, M.H., Oh, S., 2015. Modeling stream-aquifer interactions under seasonal
597 groundwater pumping and managed aquifer recharge. Groundwater, 57 (2), 216–225. doi:
598 10.1111/gwat.12799
- 599 Lelièvre, R.F., 1969. Study of the influence of pumping in alluvial aquifers on the base flow
600 of rivers – in French (Etude de l'influence de pompages en nappes alluviales sur le régime
601 d'étiage du réseau superficiel). Report BRGM 69 SGL 073 HYD., 95 p.

- 602 Manglik, A., Rai, S.N., Singh, R.N., 1997. Response of an unconfined aquifer induced by
603 time varying recharge from a rectangular basin. *Water Resources Management*, 11, 185–196.
- 604 Manglik, A., Rai, S.N., Singh, R.N., 2004. Modelling of aquifer response to time varying
605 recharge and pumping from multiple basins and wells. *Journal of Hydrology* 292, 23–29.
- 606 Marino, M.A., 1967. Hele-Shaw model study of the growth and decay of groundwater ridges.
607 *Journal of Geophysical Research*, 72, 4, 1195-1205.
- 608 Marino, M.A., 1974. Growth and decay of groundwater mounds induced by percolation.
609 *Journal of Hydrology* 22, 295-301.
- 610 Marino, M.A., 1975. Artificial groundwater recharge, i. Circular recharging area. *Journal of*
611 *Hydrology* 25, 201-208.
- 612 Massuel, S., Perrin, J., Mascré, C., Mohamed, W., Boisson, A., Ahmed, S., 2014. Managed
613 aquifer recharge in South India: What to expect from small percolation tanks in hard rock?
614 *Journal of Hydrology*, 512, 157–167. <https://doi.org/10.1016/j.jhydrol.2014.02.062>.
- 615 Moench, A.F., 1996. Flow to well in a water-table aquifer: an improved Laplace transform
616 solution. *Ground Water*, 34 (4), 593-596.
- 617 Molden, D., Sunada, D.K., Warner, J.W., 1984. Microcomputer model of artificial recharge
618 using Glover's solution. *Ground Water*, Jan.-Feb. 1984, 73-79.
- 619 Neuman, S.P., 1972. Theory of flow in unconfined aquifers considering delayed response of
620 the water table. *Water Resources Research*, 8, no. 4: 1031-1045.
- 621 Nicolas, M., Bour, O., Selles, A., Dewandel, B., Bailly-Comte, V., Chandra, S., Ahmed, S.,
622 Maréchal, J.-C., 2019. Managed aquifer recharge in fractured crystalline rock aquifers: Impact
623 of horizontal preferential flow on recharge dynamics. *Journal of Hydrology* 573, 717–732.
624 <https://doi.org/10.1016/j.jhydrol.2019.04.003>.
- 625 Polubarinova-Kochina, P.Y. 1977. *Theory of Ground Water Movement*. Moscow: Nauka, in
626 Russian. 665 p.
- 627 Rao, N.H., Sarma, P.B.S., 1981. Ground-water recharge from rectangular areas: *Ground*
628 *Water*, 19, no. 3, 270–274.
- 629 Rao, N.H., Sarma, P.B.S., 1984. Recharge to aquifers with mixed boundaries. *Journal of*
630 *Hydrology*, 74, 43-51.
- 631 Rai, S.N., Singh, R. N., 1996. On the prediction of groundwater mound formation due to
632 transient recharge from a rectangular area. *Water Resources Management*, 10: 189-198.
- 633 Rai, S.N., Ramana, D.V., Singh, R.N., 1998. On the prediction of ground-water mound
634 formation in response to transient recharge from a circular basin. *Water Resources*
635 *Management* 12, 271–284.
- 636 Rai, S.N., Ramana, D.V., Thiagarajan, S., Manglik, A., 2001. Modelling of groundwater
637 mound formation resulting from transient recharge. *Hydrol. Process.* 15, 1507–1514. DOI:
638 10.1002/hyp.222

- 639 Stafford, N., Che, D., Mays, L.W., 2015. Optimization model for the design of infiltration
640 basins. *Water Resources Management*, 29, 2789–2804. DOI 10.1007/s11269-015-0970-6
- 641 Theis, C.V., 1935. The relation between the lowering of the piezometric surface and the rate
642 and duration of discharge of a well using groundwater storage. *Transactions of the American*
643 *Geophysical Union*, 16, 519–524.
- 644 Theis, C.V., 1941. The effect of a well on the flow of a nearby stream. *Transactions of the*
645 *American Geophysical Union*, 22, 734–738.
- 646 Ward, N.D., Lough, H., 2011. Stream depletion from pumping a semiconfined aquifer in a
647 two-layer leaky aquifer system. *Journal of Hydrologic Engineering*, 16 (11), 955-959.
- 648 Warner, J.W., Molden, D., Mondher, C., D.K. Sunada, 1989, Mathematical analysis of
649 artificial recharge from basins: *Water Resources Bulletin*, 25 (2), 401–411.
- 650 Yihdego, Y., 2017. Simulation of groundwater mounding due to irrigation practice: case of
651 wastewater reuse engineering design, *Hydrology*, 4, 19, 1-10. doi:10.3390/hydrology4020019
- 652 Zlotnik, V.A., Kacimov, A., Al-Maktoumi, A., 2017. Estimating groundwater mounding in
653 sloping aquifers for managed aquifer recharge. *Ground Water*, 55 (6), 797-810. doi:
654 10.1111/gwat.12530
- 655 Zomorodi, K., 2005. Simplified solutions for groundwater mounding under stormwater
656 infiltration facilities: *Proceedings of the American Water Resources Association 2005 annual*
657 *Water Resources Conference*, November 7–10, 2005, Seattle, Washington, 4 p.
- 658

659

APPENDICES

660 **Appendix A.**

661 A-1. Groundwater flow of groundwater mounding for a rectangular basin with a uniform
662 percolation rate (Fig.2) is defined by the following nonlinear Boussinesq equation:

$$663 \quad \frac{\partial}{\partial x} \left(Kh \frac{\partial h}{\partial x} \right) + \frac{\partial}{\partial y} \left(Kh \frac{\partial h}{\partial y} \right) + R = S \frac{\partial h}{\partial t} \quad \text{A-1}$$

664 With K the hydraulic conductivity of the aquifer, S the aquifer storativity and R the recharging
665 rate.

666 Boundary conditions are $h(x, y, 0) = h_0$; $h(\pm\infty, y, t) = h(x, \pm\infty, t) = h_0$

667 Defining $Z = h^2 - h_0^2$, and assuming a homogeneous and isotropic aquifer ($K=\text{constant}$),
668 Hantush (1967) obtained the following approximate partial differential equation:

$$669 \quad \frac{\partial^2 Z}{\partial x^2} + \frac{\partial^2 Z}{\partial y^2} + \frac{2R}{K} = \frac{1}{v} \frac{\partial Z}{\partial t} \quad \text{A-2}$$

670 with $h-h_0 < 0.5h_0$, $v = \frac{K\bar{b}}{S}$, \bar{b} is a constant of linearization $\bar{b} = \frac{1}{2}(h_0 + h_t)$.

671 Boundary conditions: $Z(x, y, 0) = 0$; $Z(\pm\infty, y, t) = Z(x, \pm\infty, t) = 0$; $\frac{\partial Z(0, y, t)}{\partial x} = \frac{\partial Z(x, 0, t)}{\partial y} = 0$

672

673 A-2. Hantush's approximate partial differential equation for a well pumping an unconfined,
674 infinite and horizontal aquifer (Hantush, 1964, 1965).

$$675 \quad \frac{\partial^2 Z}{\partial x^2} + \frac{\partial^2 Z}{\partial y^2} = \frac{1}{v} \frac{\partial Z}{\partial t} \quad \text{A-3}$$

676 $Z = h^2 - h_0^2$, with $h_0 - h < 0.5h_0$

677 Boundary conditions:

678 $Z(x, y, 0) = 0$; $Z(\pm\infty, y, t) = Z(x, \pm\infty, t) = 0$; $\lim_{r \rightarrow 0} r \frac{\partial Z}{\partial r} = \frac{Q_{Pump}}{\pi K}$

679 Q_{Pump} is the pumping rate (<0) and r the distance to the pumping well.

680

681 **Appendix B.**

682 Integration of Eq. 1 into a rectangular surface of lengths $2x_L \times 2y_L$ and considering that the
683 recharging rate, R , is uniformly distributed on the rectangular recharging area ($2x_L \times 2y_L$), i.e.

684 $R = \frac{Q_{Rech}}{4x_L y_L}$, Eq.2 becomes:

$$Z_{Rech}(x_{obs}, y_{obs}, t) = h^2 - h_0^2 = \frac{R}{2\pi K} \int_{-x_L}^{+x_L} \int_{-y_L}^{+y_L} W \left(\frac{(x - x_{obs})^2 + (y - y_{obs})^2}{4vt} \right) dx dy$$

685

B-1

686 Then, because of the properties of exponential integrals [$W\left(\frac{a}{t}\right) = \int_{a/t}^{\infty} \frac{e^{-y}}{y} dy = \int_0^t \frac{e^{-a/\tau}}{\tau} d\tau$],
 687 it follows

$$Z_{Rech}(x_{obs}, y_{obs}, t) = \frac{R}{2\pi K} \int_{-x_L}^{+x_L} \int_{-y_L}^{+y_L} \int_0^t \frac{e^{\frac{-(x-x_{obs})^2-(y-y_{obs})^2}{4v\tau}}}{\tau} d\tau dx dy$$

688 B-2

689 According to the Fubini theorem (i.e. t , x and y are independent variables), the order of
 690 integration can be inverted, resulting in:

$$Z_{Rech}(x_{obs}, y_{obs}, t) = \frac{R}{2\pi K} \int_0^t \underbrace{\int_{-x_L}^{+x_L} \frac{e^{\frac{-(x-x_{obs})^2}{4v\tau}}}{\sqrt{\tau}} dx}_{(a)} \underbrace{\int_{-y_L}^{+y_L} \frac{e^{\frac{-(y-y_{obs})^2}{4v\tau}}}{\sqrt{\tau}} dy}_{(b)} d\tau$$

691 B-3

692
 693 Performing a change of variable $\vartheta = \frac{(x-x_{obs})}{2\sqrt{v\tau}}$, the (a) term in Eq. B-3 can be rewritten as:

$$\int_{-x_L}^{+x_L} \frac{e^{\frac{-(x-x_{obs})^2}{4v\tau}}}{\sqrt{\tau}} dx = \int_{-(x_L+x_{obs})/2\sqrt{v\tau}}^{(x_L-x_{obs})/2\sqrt{v\tau}} 2\sqrt{v} e^{-\vartheta^2} d\vartheta$$

694 B-4

695 The right part in Eq. B-4 can be separated into two terms related to the *Erf* function

696 [$\int_a^b e^{-u^2} du = \frac{\sqrt{\pi}}{2} [Erf(u)]_a^b = \frac{\sqrt{\pi}}{2} (Erf(b) - Erf(a))$], therefore:

$$\int_{-(x_L+x_{obs})/2\sqrt{v\tau}}^{(x_L-x_{obs})/2\sqrt{v\tau}} 2\sqrt{v} e^{-\vartheta^2} d\vartheta = \sqrt{\pi v} \left[Erf\left(\frac{x_L+x_{obs}}{2\sqrt{v\tau}}\right) + Erf\left(\frac{x_L-x_{obs}}{2\sqrt{v\tau}}\right) \right]$$

697 B-5

698 Changing the variable $\vartheta' = \frac{(y-y_{obs})}{2\sqrt{v\tau}}$ on term (b) in Eq. B-3, and using the same procedure as
 699 described before, the (b) term can be rewritten

$$\int_{-y_L}^{+y_L} \frac{e^{\frac{-(y-y_{obs})^2}{4v\tau}}}{\sqrt{\tau}} dy = \sqrt{\pi v} \left[Erf\left(\frac{y_L+y_{obs}}{2\sqrt{v\tau}}\right) + Erf\left(\frac{y_L-y_{obs}}{2\sqrt{v\tau}}\right) \right]$$

700 B-6

701 Finally, combining equations B-5 and B-6, and since $\nu = \frac{K\bar{b}}{S}$, we obtain:

$$Z_{Rech}(x_{obs}, y_{obs}, t) = h^2 - h_o^2$$

$$= \frac{R\bar{b}}{2S} \int_0^t \left[\operatorname{Erf}\left(\frac{x_L + x_{obs}}{2\sqrt{\nu\tau}}\right) + \operatorname{Erf}\left(\frac{x_L - x_{obs}}{2\sqrt{\nu\tau}}\right) \right] \times \left[\operatorname{Erf}\left(\frac{y_L + y_{obs}}{2\sqrt{\nu\tau}}\right) + \operatorname{Erf}\left(\frac{y_L - y_{obs}}{2\sqrt{\nu\tau}}\right) \right] d\tau$$

702 B-7

703 Equation B-7 demonstrates that the well solution for an unconfined and isotropic aquifer
 704 (Hantush, 1964a, 1965) integrated into a rectangular plane is exactly the same as Hantush's
 705 analytical solution for a rectangular recharging area with a uniform distribution of the
 706 recharge flux (Eq. 13 in Hantush, 1967).

707

708 **Appendix C.**

709 The hydraulic-head solution for a rectangular recharging area and a pumping well between
 710 two parallel boundaries (constant head or no-flow boundary).

711 x_w and y_w : coordinates of the pumping well, d : the distance between the centre of the
 712 recharging area and the stream. $2L$ is the distance between both limits. $x=y=0$ at the centre of
 713 the recharging area. $\nu = \frac{K\bar{b}}{S}$. Below are presented the general solutions for hydraulic head
 714 between two parallel limits; b and c are coefficients, b or $c=1$ for a no-flow boundary, and b
 715 or $c=-1$ for is a constant-head boundary (Dirichlet's condition).

716

717

718

719

720

721

722

723

724

725 Term for the pumping well:

$$\begin{aligned}
 Z_{2Limit_Pump}(x_{obs}, y_{obs}, t) &= h^2 - h_o^2 \\
 &= \frac{Q}{2\pi K} \left\{ W \left(\frac{(x_{obs} - x_w)^2 + (y_{obs} - y_w)^2}{4vt} \right) \right. \\
 &\quad + \sum_{n=0,2,4..}^{\infty} b^{n/2+1} c^{n/2} W \left(\frac{(2nL + 2d - x_{obs} + x_w)^2 + (y_{obs} - y_w)^2}{4vt} \right) \\
 &\quad + \sum_{n=2,4..}^{\infty} (bc)^{n/2} W \left(\frac{(-2nL - x_{obs} + x_w)^2 + (y_{obs} - y_w)^2}{4vt} \right) \\
 &\quad + \sum_{n=2,4..}^{\infty} (bc)^{n/2} W \left(\frac{(2nL - x_{obs} + x_w)^2 + (y_{obs} - y_w)^2}{4vt} \right) \\
 &\quad \left. + \sum_{n=2,4..}^{\infty} b^{n/2-1} c^{n/2} W \left(\frac{(-2nL + 2d - x_{obs} + x_w)^2 + (y_{obs} - y_w)^2}{4vt} \right) \right\}
 \end{aligned}$$

726 Eq. C-1

727

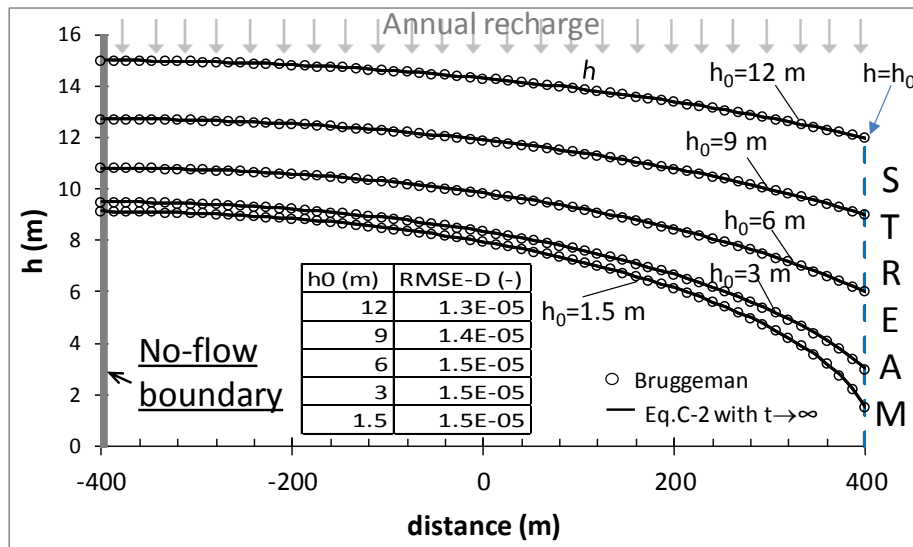
728 Term for the rectangular recharging area:

$$\begin{aligned}
 Z_{2Limit_Rech}(x_{obs}, y_{obs}, t) &= h^2 - h_o^2 \\
 &= \frac{R\bar{b}}{2S} \left\{ \int_0^t \left[\operatorname{Erf} \left(\frac{x_L + x_{obs}}{2\sqrt{v\tau}} \right) + \operatorname{Erf} \left(\frac{x_L - x_{obs}}{2\sqrt{v\tau}} \right) \right] \times \left[\operatorname{Erf} \left(\frac{y_L + y_{obs}}{2\sqrt{v\tau}} \right) + \operatorname{Erf} \left(\frac{y_L - y_{obs}}{2\sqrt{v\tau}} \right) \right] d\tau \right. \\
 &\quad + \sum_{n=0,2,4..}^{\infty} b^{n/2+1} c^{n/2} \int_0^t \left[\operatorname{Erf} \left(\frac{x_L + 2nL + 2d - x_{obs}}{2\sqrt{v\tau}} \right) + \operatorname{Erf} \left(\frac{x_L - 2nL - 2d + x_{obs}}{2\sqrt{v\tau}} \right) \right] \\
 &\quad \times \left[\operatorname{Erf} \left(\frac{y_L + y_{obs}}{2\sqrt{v\tau}} \right) + \operatorname{Erf} \left(\frac{y_L - y_{obs}}{2\sqrt{v\tau}} \right) \right] d\tau \\
 &\quad + \sum_{n=2,4..}^{\infty} (bc)^{n/2} \int_0^t \left[\operatorname{Erf} \left(\frac{x_L - 2nL - x_{obs}}{2\sqrt{v\tau}} \right) + \operatorname{Erf} \left(\frac{x_L + 2nL + x_{obs}}{2\sqrt{v\tau}} \right) \right] \\
 &\quad \times \left[\operatorname{Erf} \left(\frac{y_L + y_{obs}}{2\sqrt{v\tau}} \right) + \operatorname{Erf} \left(\frac{y_L - y_{obs}}{2\sqrt{v\tau}} \right) \right] d\tau \\
 &\quad + \sum_{n=2,4..}^{\infty} (bc)^{n/2} \int_0^t \left[\operatorname{Erf} \left(\frac{x_L + 2nL - x_{obs}}{2\sqrt{v\tau}} \right) + \operatorname{Erf} \left(\frac{x_L - 2nL + x_{obs}}{2\sqrt{v\tau}} \right) \right] \\
 &\quad \times \left[\operatorname{Erf} \left(\frac{y_L + y_{obs}}{2\sqrt{v\tau}} \right) + \operatorname{Erf} \left(\frac{y_L - y_{obs}}{2\sqrt{v\tau}} \right) \right] d\tau \\
 &\quad + \sum_{n=2,4..}^{\infty} b^{n/2-1} c^{n/2} \int_0^t \left[\operatorname{Erf} \left(\frac{x_L - 2nL + 2d - x_{obs}}{2\sqrt{v\tau}} \right) + \operatorname{Erf} \left(\frac{x_L + 2nL - 2d + x_{obs}}{2\sqrt{v\tau}} \right) \right] \\
 &\quad \left. \times \left[\operatorname{Erf} \left(\frac{y_L + y_{obs}}{2\sqrt{v\tau}} \right) + \operatorname{Erf} \left(\frac{y_L - y_{obs}}{2\sqrt{v\tau}} \right) \right] d\tau \right\}
 \end{aligned}$$

729 Eq. C-2

730 The graph below compares the solution Eq. C-2 with $b=-1$, $c=1$, $2x_L=2L$, $d=L$, $y_L \rightarrow \infty$ and
 731 $t \rightarrow \infty$, to Bruggeman's steady-state solution (1999; sol. 21.11, p.24). This case corresponds to
 732 the hydraulic-head profile caused by recharge from precipitation (R) through an infinite strip
 733 of width $2L$ bounded on one side by a stream and on the other by a no-flow boundary. Aquifer
 734 parameters are: $K=10^{-4}$ m/s, $S=0.05$, $2L=800$ m, $R=1.27 \times 10^{-8}$ m/s (or 400 mm/year), and h_o

735 varying from 1.5 to 12 m. The insert shows standardized Root Mean Square Error values
 736 (RMSE-D) for the five cases.



737

738 **Appendix D.**

739 The hydraulic-head solution for a pumping well near a stream with a partially clogged
 740 streambed that partially penetrates the aquifer (Hunt, 1999), modified for an unconfined
 741 condition (linearized Boussinesq solution as in Hantush 1967) is:

$$Z_{HuntPump}(x_{obs}, y_{obs}, t) = h^2 - h_o^2 = \frac{Q_{Pump}}{2\pi K} \left[W \left(\frac{x_{obs}^2 + y_{obs}^2}{4vt} \right) - \int_0^\infty e^{-\theta W} \left(\frac{(d + |d - x_{obs}| + 2K\bar{b}\theta/\lambda)^2 + y_{obs}^2}{4vt} \right) d\theta \right]$$

742

Eq. D-1

743 with $\lambda = \frac{b}{b''} k''$; b : stream width, b'' : streambed thickness and k'' : streambed hydraulic
 744 conductivity.

745 The right part of Eq. D-1 can be rearranged with the following change of variable

746 $\theta = -Ln(u)$ then $= -\frac{1}{u} du$; Ln = natural logarithm.

747 Then Eq. D-1 becomes:

$$Z_{HuntPump}(x_{obs}, y_{obs}, t) = h^2 - h_o^2 = \frac{Q}{2\pi K} \left[W \left(\frac{x_{obs}^2 + y_{obs}^2}{4vt} \right) - \int_0^1 W \left(\frac{(d + |d - x_{obs}| - 2K\bar{b}Ln(u)/\lambda)^2 + y_{obs}^2}{4vt} \right) du \right]$$

748

Eq. D-2

749

750 **Figure captions**

751 Figure 1. Conceptual models of the theoretical examples presented. a) Recharging and
 752 pumping an isotropic aquifer near a stream (Dirichlet's condition). b) Recharging and
 753 pumping an isotropic aquifer limited in space by a stream (Dirichlet's condition) and a no-
 754 flow boundary (strip aquifer), with and without the influence of natural recharge. c)
 755 Recharging and pumping an aquifer near a stream with a clogged streambed that partially
 756 penetrates the aquifer. d) Recharging an unconfined and isotropic top layer aquifer and
 757 pumping a bottom semi-confined aquifer.

758

759 Figure 2. Definition sketch (plan and section views) of the Hantush's (1967) conceptual
 760 model of groundwater mounding from a rectangular recharging area.

761 Figure 3. Definition sketch of: a) recharging and pumping an isotropic aquifer near a stream,
 762 b) recharging and pumping an isotropic aquifer limited in space by a stream (Dirichlet's
 763 condition) and a no-flow boundary (strip aquifer). Similar to Figs. 1a and b.

764

765 Figure 4. Hydraulic-head profiles after 60 days (a and c), and impacts on streamflow rate (b
 766 and d; <0: decrease of streamflow rate and >0: increase). a) and b) Recharging and pumping
 767 an isotropic aquifer near a stream (refer to Figs. 1a and 3a). c) and d) Recharging and
 768 pumping an isotropic aquifer limited in space by a river and a no-flow boundary (strip aquifer,
 769 refer to Figs. 1b and 3b). $K=10^{-4}$ m/s, $S= 0.05$, $h_0=12$ m, $x_L=y_L=40$ m, $R=2.96 \times 10^{-6}$ m/s and
 770 $Q_{Pump}=17$ m³/h.

771

772 Figure 5. Recharging and pumping an isotropic aquifer limited in space by a stream and a no-
 773 flow boundary (strip aquifer) with the influence of natural recharge, hydraulic head profiles.
 774 a) Without pumping, in this case the solution is identical Bruggeman (1999) solution
 775 (standardized RMSE= 2.22×10^{-5} m). b) With a recharging area and a pumping well at 140 m
 776 from the centre of the recharging area after 1 day and 60 days of recharging and pumping.
 777 $K=10^{-4}$ m/s, $S= 0.05$, $h_0=12$ m, $x_L=y_L=40$ m, $R=2.96 \times 10^{-6}$ m/s, $Q_{Pump}=17$ m³/h and
 778 $R_{NatRech}=1.27 \times 10^{-8}$ m/s.

779

780 Figure 6. Recharging and pumping an isotropic aquifer near a stream that partially penetrates
 781 the aquifer with clogged streambed (Fig. 1c). a) Hydraulic head profile after 60 days. b)

782 Impact on streamflow rate, for various stream-leakance coefficients ($\lambda = \infty, 10^{-4}, 5 \cdot 10^{-5}, 10^{-5},$
783 $5 \cdot 10^{-6}$ and 10^{-6} m/s). Stream width: 10 m, $K=10^{-4}$ m/s, $S=0.05$, $h_0=12$ m, $x_L=y_L=40$ m,
784 $R=2.96 \cdot 10^{-6}$ m/s and $Q_{Pump}=17$ m³/h.

785

786 Figure 7. Multi-aquifer system, recharging the top aquifer and pumping the deepest one. a)
787 Hydraulic-head profiles in the upper aquifer and b) drawdown of water level in the deeper
788 aquifer after 1 day and 60 days. c) Total drainage flow-rate induced by the recharging area
789 and by the pumping well, compared to the case with the recharging area only (without
790 pumping well). $K_1=10^{-4}$ m/s, $S_1=0.05$, $h_0=12$ m, $T_2=10^{-4}$ m²/s, $S_2=10^{-3}$, $k'/e'=5 \cdot 10^{-7}$ m²/s,
791 $x_L=y_L=40$ m, $R=2.96 \cdot 10^{-6}$ m/s and $Q_{Pump}=17$ m³/h.

792

793

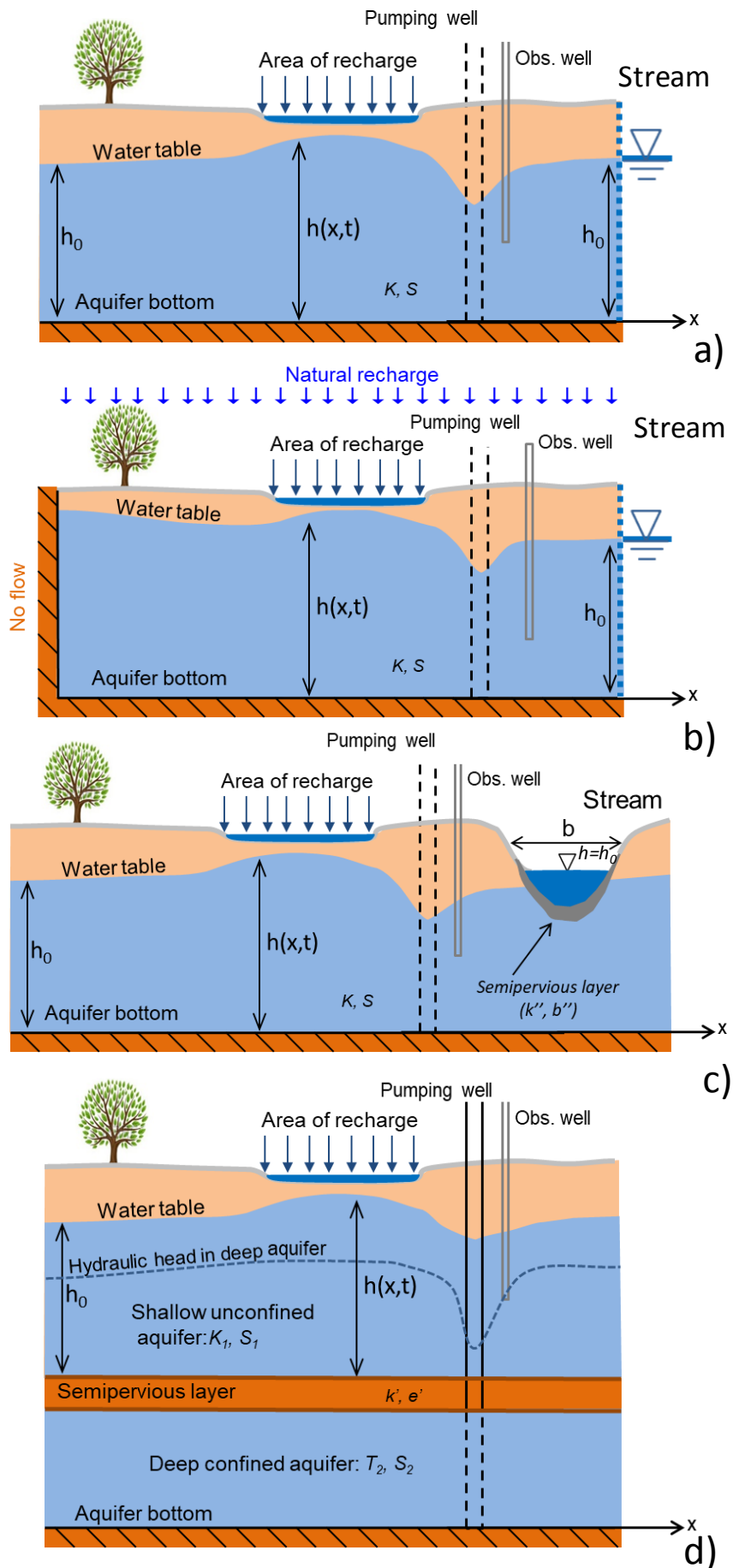


Fig.1

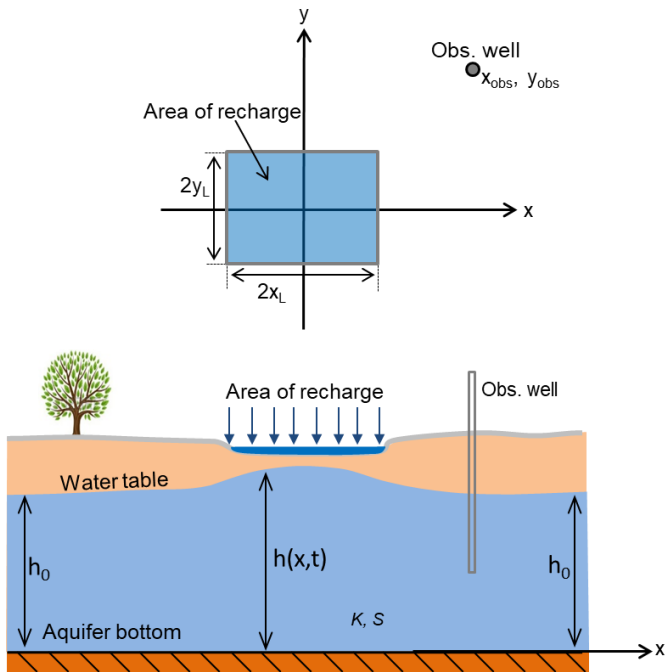


Fig.2

795

796

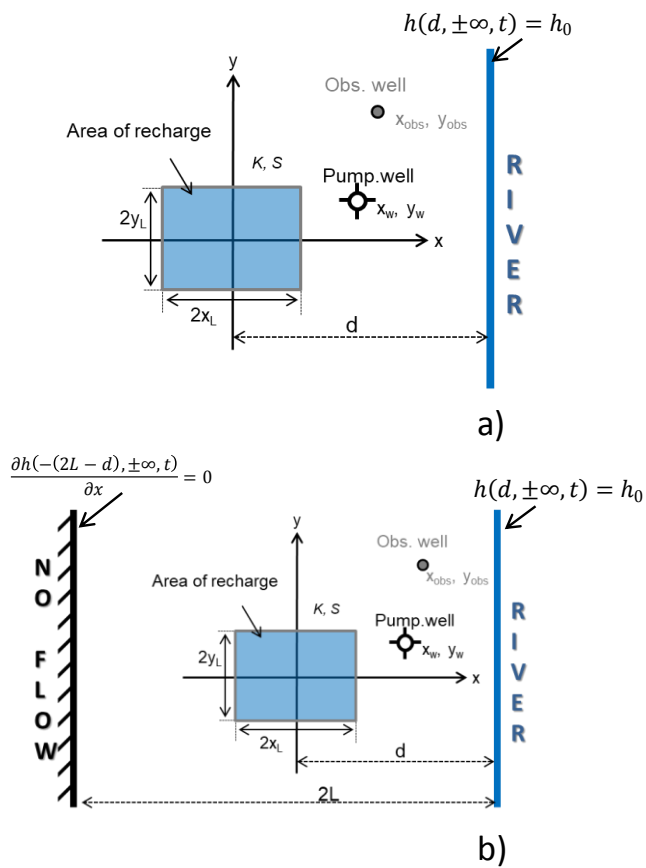


Fig.3

797

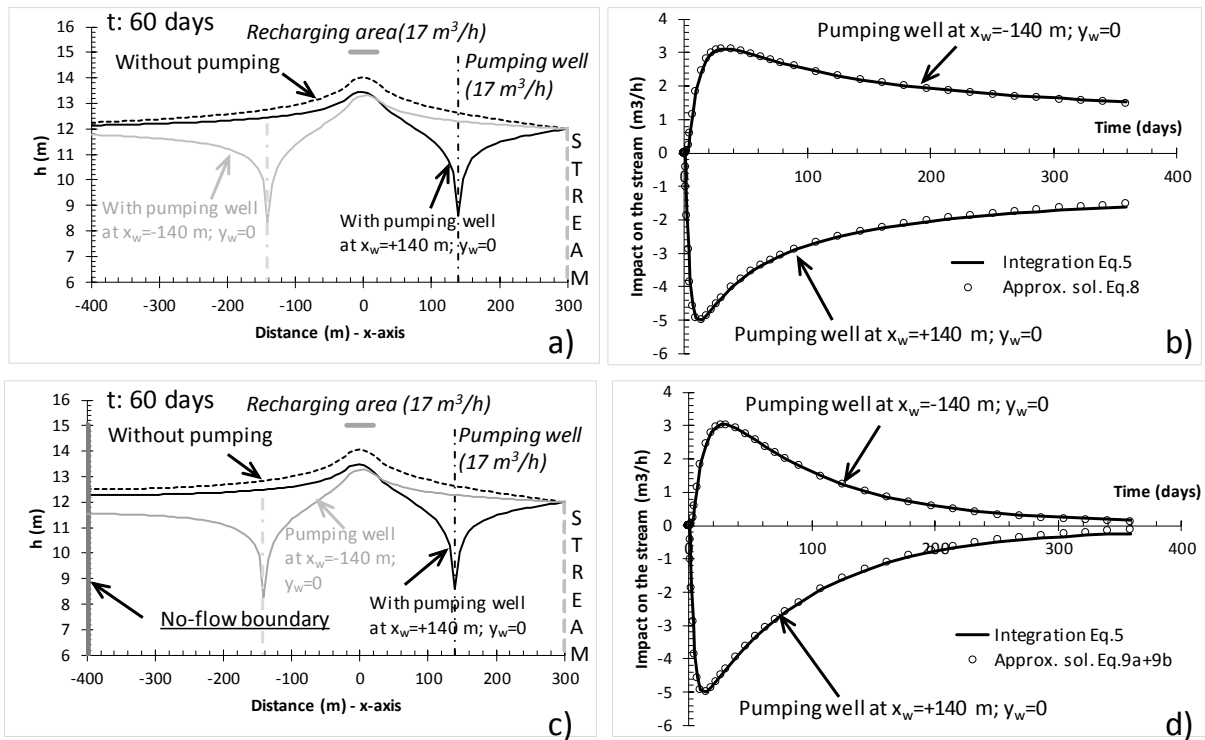


Fig.4

798

799

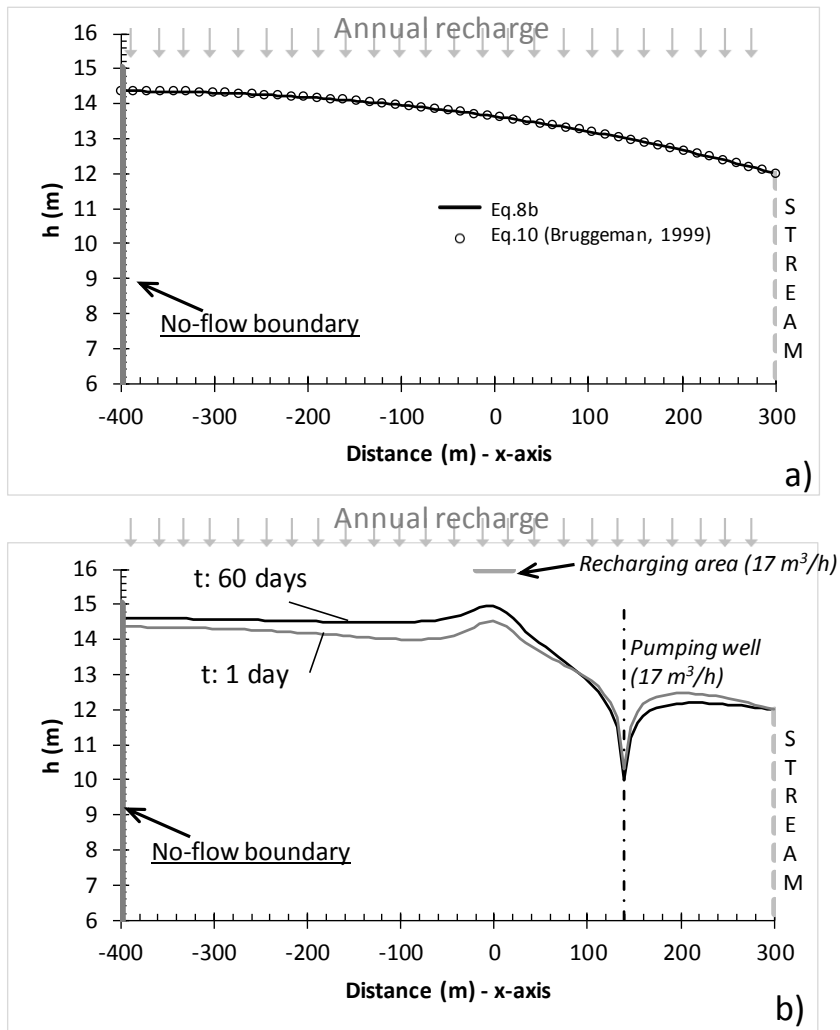


Fig.5

800
801
802
803

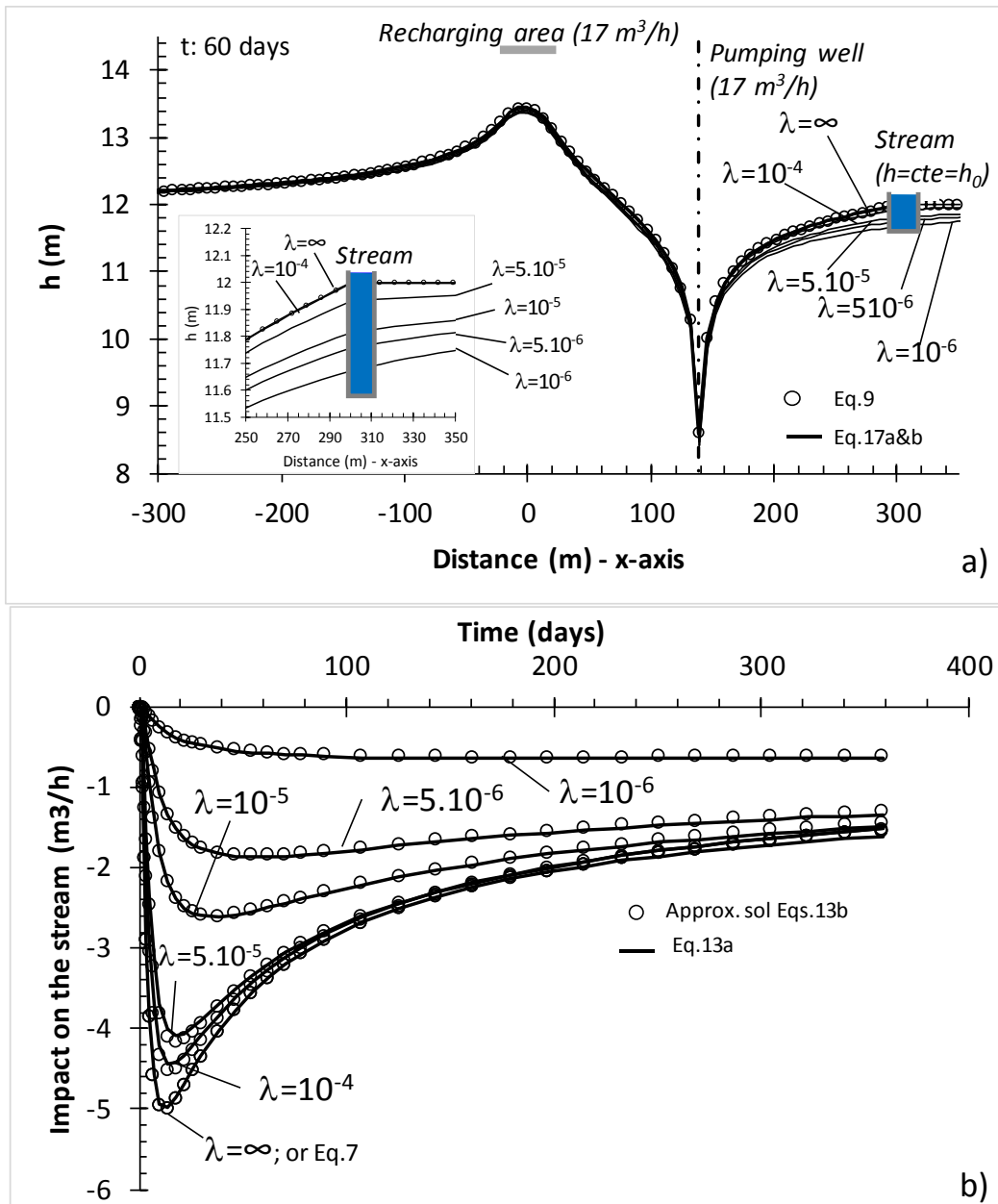


Fig.6

804

805

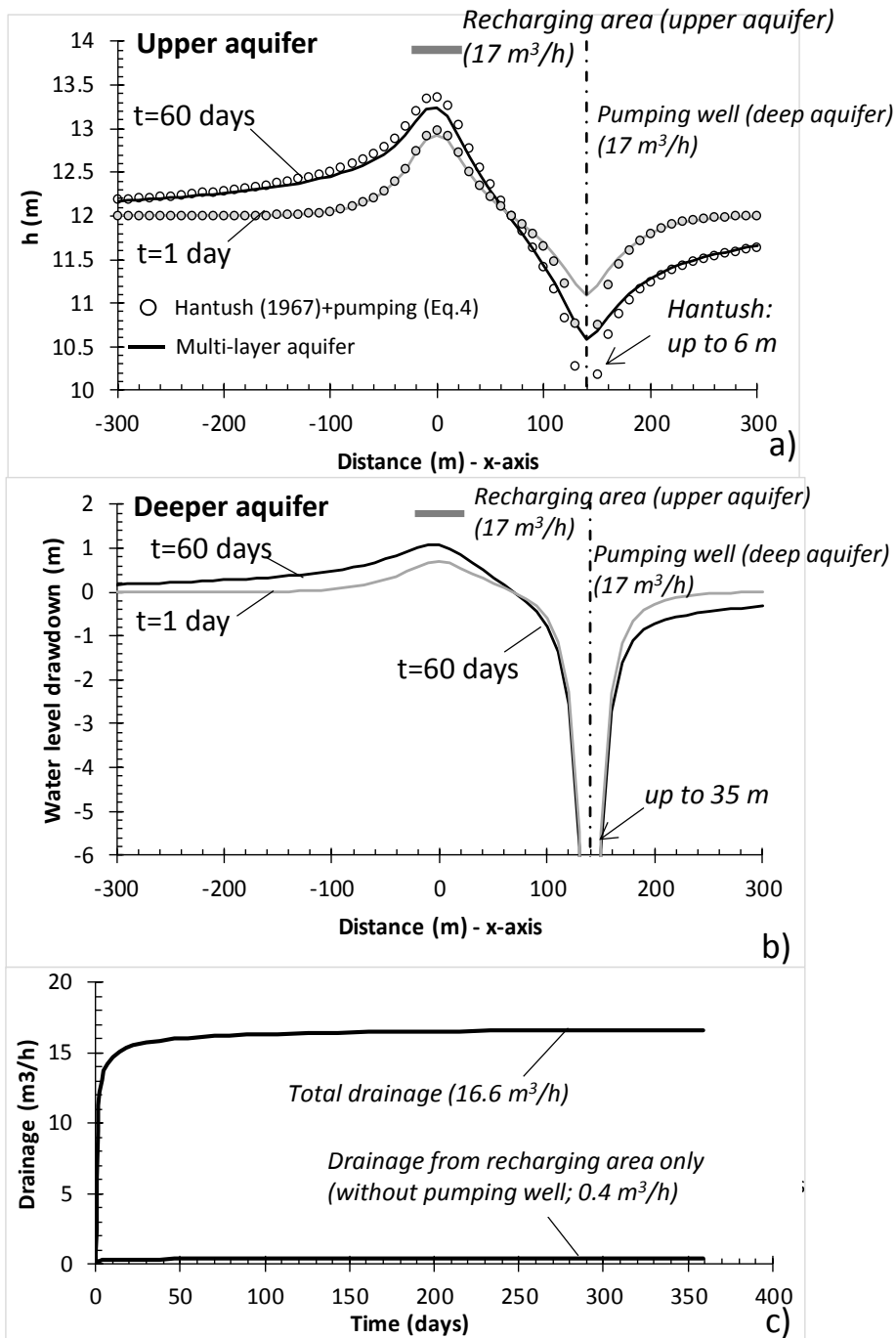


Fig.7

806

807